J Opt (September 2021) 50(3):495–501
https://doi.org/10.1007/s12596-021-00728-5

RESEARCH ARTICLE

Composite optical interference in non-unitary and unitary beam-splitter systems

Zhikai Li[1] · Yulin Wang[1] · Tao Li[2] · Chengping Huang[1] · Yong Zhang[1]

Received: 6 February 2021 / Accepted: 15 June 2021 / Published online: 13 July 2021

Abstract In this paper, we theoretically propose and demonstrate a non-unitary beam-splitter (BS) by introducing coupling losses at the interface of the plasmonic waveguide and multimode dielectric waveguide (DW). The coupling losses enable us to modify the reflection and transmission factors, which can result in arbitrary shift of interference curves of two outputs. Specially, the lossy non-unitary BS can tune the amplitudes and phases of two outputs, even making them change synchronously, regardless of input phase differences. After a $\pi/2$ phase delay in one arm, these two outputs are fed into another multimode DW. This DW is a normal unitary BS, working like the Michelson interferometer, where anti-synchronous interference can take place. At last, the whole device outputs an invariant zero energy state in one port, exhibiting a phase-insensitive performance. Our study provides a versatile design platform to realize non-unitary/unitary BS and construct more multi-functional devices.

Keywords Beam-splitter · Interference · Plasmonic waveguide · Coupling losses

✉ Yulin Wang
yulinwang@njtech.edu.cn

[1] Department of Physics, Nanjing Tech University, Nanjing 210009, China

[2] College of Engineering and Applied Sciences, Nanjing University, Nanjing 210093, China

Introduction

Beam-splitter(BS) is a fundamental component of information optical systems. Usually, in a geometrically optical scale typical BS is in macroscopical scale. With the improvement of micro-nano fabrication methods, the scale of beam splitters has been developed from macroscopic to on-chip integration, it is usually used in silicon-based waveguides [1–3], photonic crystals [4–6], plasmonic systems [7–10], metamaterials [11–14], etc. Functionally, BS is generally used for splitting optical beams [15–18]and classical optical interference [19–22]. In recent years, some quantum interferences [23–26] and PT symmetric systems [27, 28] have also been reported taking advantage of BS. Among all the usages, BS is more commonly used for interference purposes.

Typically, Michelson interferometer is a lossless system with a BS featuring unitary transformation and Hermitian evolution of light. While considering losses in BS, it may enable us to modify the phase factors of the reflection and transmission coefficients, and the BS is non-unitary [28, 29]. Recently, an unconventional anti-coalescence has been demonstrated for interference between two single plasmons in a non-unitary BS system [29]. Besides, the non-unitary BS system has also been realized in magnon-photon interference in an atomic ensemble [30]. In previous work, two kinds of classical optical BSs have been realized in a plasmonic switch (2×2 inputs and outputs) composed of metallic strip waveguides [31]. A conventional interference pattern was observed as a complete oscillation due to the energy conservation law (two outputs exhibit sinusoidal curves with maximum intensity in one output and minimum intensity in the other). We call it anti-synchronous interference. Besides, a non-unitary interference pattern was also observed, where the two output

curves show an arbitrary phase shift. In one special case, two outputs are correlated that their amplitudes tend to reach extreme values simultaneously, and the phase difference is zero, which is named as synchronous interference. In such synchronous interference, the amplitudes change synchronously, and the phases keep locked. Compared with the anti-synchronous interference, the synchronous one is more critical and difficult to obtain.

In this work, we theoretically propose and demonstrate a synchronous interference in a 2×2 hybrid plasmonic waveguide with directional coupling function, which extends non-unitary BS to a more general waveguide system. Any splitting ratio with one input can be achieved according to multimode interference (MMI) theory. Moreover, the coupling losses enable us to modify the reflection and transmission factors, which can result in arbitrary shift of interference curves of two outputs, even make two interference curves change simultaneously. When cascading it to another 2×2 dielectric waveguide (DW), which provides a unitary BS with an anti-synchronous interference, we finally achieve a favorable phase-insensitive interference device, where one of the outputs maintains zero energy state. Since the device still has a non-zero output for the single input, which indicates it may work as a phase-insensitive XOR logical gate. Our study provides a versatile design platform to realize non-unitary/unitary BS and construct multi-functional devices.

Anti-synchronous interference in lossless unitary BS

Here, we would like first to introduce the anti-synchronous interference device, which can be easily realized in a transmission-reflection process with a half-to-half unitary BS [19, 20, 31]. Now, we extend it to a more integratable DW system with 2×2 input and output ports. For simplicity, all the waveguides are designed as the dielectric planar waveguide of Al_2O_3 ($n_{AO} = 1.7$). The center waveguide is thick enough to accommodate more than two transverse magnetic (TM) modes to support MMI [32, 33], exhibiting self-imaging property of the optical field. Based on the MMI theory, the field amplitudes and phases will recover with a period of $\frac{M}{N} \times \frac{3L_c}{a}$. Here, $L_c = \pi/\Delta\beta$ is the beat length of two lowest-order modes, $\Delta\beta$ is the corresponding mismatch of the propagation wave-vector. M and N are any positive integers without a common divisor, N is the number of self-images, and M defines several possible device lengths with N images. Especially, a 2×2 restricted MMI coupler has $a = 3$. Thus, when the center waveguide length is set as $M \times L_c$, the single input signal will transport to one of the two output ports, revealing cross coupling and corresponding to directional coupling function. If the length is $M/2 \times L_c$, the optical field from the single input will generate double images in the two outputs, inducing a half-to-half splitting.

Full wave simulations are carried out by a commercial FEM solution of COMSOL (v4.2a) with the working wavelength of 850 nm. Besides, all the design solutions here are also suitable to other wavelengths. Considering the applications of optical communication, the working wavelength of 850 nm is applied. The thickness of center waveguide is defined as 520 nm with Al_2O_3 ($n_{AO} = 1.7$), and four-port parts are 260 nm thick for single mode. Waveguide modes from boundary mode analysis are incident into the input ports. The TM polarized wave incidents one of the input ports. According to our calculations, the coupling length L_c is about 1.02 μm. Then, a directional coupling function can be realized with the center waveguide length of 6.1 μm ($6 \times L_c$), as shown in Fig. 1a. If selecting waveguide length of 4.6 μm ($9/2 \times L_c$), we will find a considerably good half-to-half beam splitting effect (see Fig. 1b), which agrees well with our theoretical design based on 2×2 restricted MMI. Moreover, in this situation the BS can be considered as lossless, and the phase difference between two outputs is approximately equal to $\pi/2$. So when two inputs are excited simultaneously, it follows that a maximum in one channel while minimum in the other channel as expected from the energy conservation law, exhibiting a unitary BS with an anti-synchronous interference. Output interference intensities can be calculated by varying the phase difference of the two input signals, and the results are depicted in Fig. 1d, which definitely shows an obvious anti-synchronous feature with a deep interference depth of about 94.7%. However, for the case of directional coupling, we will find the interference is very weak (see Fig. 1c). It is acceptable that in a self-imaging condition, the input ports will be both re-imaged, and the optical field from different input ports will be well separated, and the overlap is very small. In this regard, using such kind of dielectric MMI waveguide system is impossible to reach a synchronous interference with a directional coupling property.

Synchronous interference in lossy non-unitary BS

In DW system, a lossless BS has been established, which features unitary transformation of light and results in an anti-synchronous interference. On the contrary, a lossy BS may enable us to modify the reflection and transmission factors. A previous study experimentally demonstrated a classical plasmonic synchronous interference depending on the conversion of surface plasmon polaritons (SPPs) from the strip mode into strongly coupled slit-mode [31].

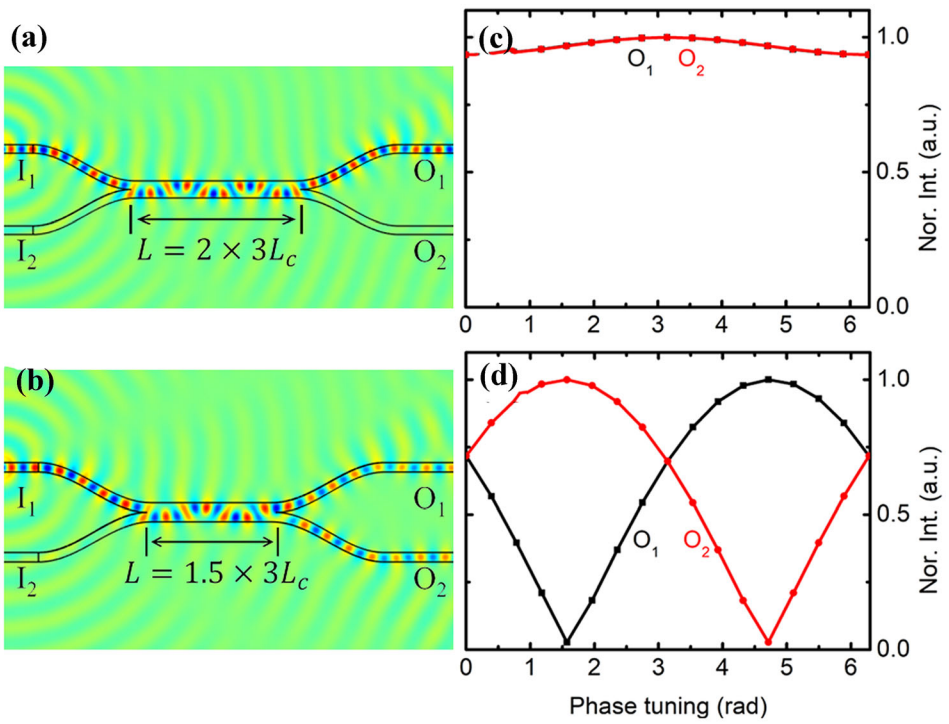

Fig. 1 The calculated MMI results for the interference distance of **a** $L = 6 \times L_c$ and **b** $L = 9/2 \times L_c$, showing directional coupling and half-to-half beam splitting properties, respectively. **c**, **d** show the corresponding interference curves of two outputs

Besides, an unconventional anti-coalescence with Hong-Ou-Mandel peak has also been observed in quantum processes [29]. It provides us a clue to find a solution to realize synchronous interference in a more generalized waveguide system with losses. In the following, we design a lossy BS by introducing an interface with a controllable coupling loss according to different mode mismatches.

Required by the synchronous interference, a non-unitary BS is designed with two combined waveguides with an interface of controllable coupling loss, where the in-phase signals can pass through while the anti-phase ones cannot. For this purpose, each of two combined waveguides has two eigenmodes. Two eigenmodes in the first waveguide are designed with a big difference in mode index. Meanwhile, one matches the connective guided mode in the second waveguide, while the other does not match and has a large coupling loss. Figure 2a schematically shows a proper mode design with two kinds of waveguide system separated with an interface. When two inputs are in the same phase, the in-phase mode (black line) M_{SPPS} can smoothly transfer to another waveguide mode M_{TM0}, while the anti-phase mode (red line) M_{SPPA} will be blocked by the interface due to the large mode mismatch. The average of the effective index of M_{SPPS} and M_{SPPA} is the beating mode M_{beat} with single port excitation, indicated by the center blue line, which has relatively small mode mismatch to both M_{TM0} and M_{TM1} modes. Therefore, it will be considerably transferred into another waveguide, possibly leading to a certain beating mode. It is a reasonable directional coupling function with synchronous interference in MMI waveguide.

Based on this theoretical scheme, we need to find out proper waveguide systems and interface with such kinds of mode properties. According to the analyses in section II, it is proved to be very difficult to realize this function in a lossless DW system. However, hybrid plasmonic and dielectric waveguides would provide a possible solution, as shown in Fig. 2c. The first metal-insulator-metal (MIM) plasmonic waveguide can support two strongly split eigenmodes, which is exactly the same as the first part of Fig. 2a. The second waveguide is a multimode DW, corresponding to the second part of Fig. 2a. The mode curves of the MIM waveguide and DW are plotted in Fig. 2b as a function of center dielectric layer thickness. The eigenequation of the TM mode in MIM waveguide is similar to three-layer dielectric slab waveguide [34]. The formula is:

$$k_0\left(\varepsilon_1 - N^2\right)^{1/2} h = m\pi + 2\arctan\left[\frac{\varepsilon_1}{\varepsilon_2}\left(\frac{N^2 - \varepsilon_2}{\varepsilon_1 - N^2}\right)^{1/2}\right] \quad (1)$$

Here h is the thickness of the center dielectric layer with permittivity of ε_1, ε_2 is the permittivity of the metal layer. k_0 is the wave vector of the vacuum, N is the effective mode index. When $m = 0$ and 1, the effective mode index of M_{SPPS} and M_{SPPA} can be obtained. According to the mode dispersion, appropriate structural parameters of two cascaded waveguides (MIM and DW) can be found to meet the requirements of the design in Fig. 2a. With the

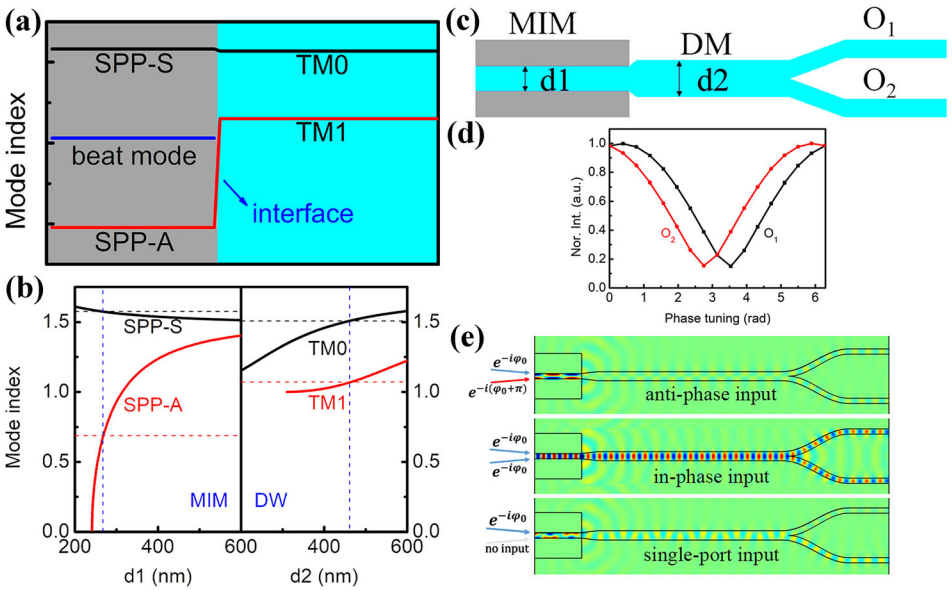

Fig. 2 **a** Assumption of mode properties of two cascaded waveguide systems, which can possibly satisfy the requirements of synchronous interference and directional coupling function. **b** Mode curves of MIM waveguide and DW as a function of center dielectric-layer thickness. **c** Schematics of lossy non-unitary BS. **d** Simulated synchronous interference results. **e** The field distributions of interferences in the conditions of the anti-phase, in-phase, and the singe-input cases (Color figure online)

optimized parameters (the middle dielectric layer of MIM is defined as SiO_2 with $n_{SO} = 1.44$ and $d_1 = 262\,\text{nm}$; the DW is defined as Al_2O_3 with $n_{AO} = 1.7$ and $d_2 = 450\,\text{nm}$), we performe a full wave simulation. Fig. 2d shows a considerably good synchronous interference. The outputs simultaneously show on-states with zero phase difference for in-phase inputs and off-states for anti-phased inputs, as depicted in the top two figures in Fig. 2e.

When two inputs are anti-phase, there will be M_{SPPA} mode in MIM waveguide. It will be prevented from propagating through the interface due to large vector mismatch between M_{SPPA} and M_{TM1}. So, destructive interference happens. While for two in-phase inputs, M_{SPPS} can smoothly transfer to M_{TM0} in the next DW, resulting in constructive interference. To confirm that, we calculate the coupling efficiency η [35] based on the mode overlap integral of $M_{\text{SPPS}}/M_{\text{TM0}}$ (for in-phase) and $M_{\text{SPPA}}/M_{\text{TM1}}$ (for anti-phase), respectively:

$$\eta = \frac{\left|\iint E_{\text{MIM}} E_{\text{DW}}\,\mathrm{d}x\,\mathrm{d}y\right|^2}{\iint |E_{\text{MIM}}|^2\,\mathrm{d}x\,\mathrm{d}y \iint |E_{\text{DW}}|^2\,\mathrm{d}x\,\mathrm{d}y} \tag{2}$$

where E_{MIM} and E_{DW} are the electric fields of MIM and DW waveguides, respectively. The XOY plane is coupling interface of the waveguide. The coupling efficiency is 61.2% for in-phase inputs, while 4.2% for anti-phase. Besides, the transmittance is also evaluated according to the S-parameter in simulation models. The transmittance are 60.3 and 4.1% of two cases. It is coincident well with coupling efficiency. Therefore, a BS of controllable loss with synchronous interference is obtained. While in the single input case, the beat mode M_{beat} will propagate through the interface and go to one of outputs with self-image property of a MMI waveguide, exhibiting a directional coupling function (see the bottom one in Fig. 2e). Thanks to directional coupling property, some logical functions may be realized.

Phase-insensitive interference in cascaded system

Based on the study on unitary/non-unitary BS, it is more interesting what will happen when we use both two kinds of BS to construct some functional devices. Figure 3a schematically illustrates the synchronous (red) and anti-synchronous (blue) interferences in a 2×2 optical systems. In the synchronous case, two output ports have simultaneous same output signals. Consequently, two equi-amplitude coherent sources with the same phase are available for the next functional process, defined by operator B_{nu}. After a 2 phase delay in one branch (operator D), they enter into the second anti-synchronous interference part (illustrated as B_u). As for the anti-synchronous one, when the input signals have a phase delay of $\pm\pi/2$, one of the modulated secondary output signals will maintain destructive interference, as schemed out in Fig. 3b. At last, the whole device outputs an invariant zero energy state in one port, exhibiting a phase-insensitive performance.

The whole transmission process of the cascaded systems can be described by transmission matrix, and the final output ports have the field intensity as follows:

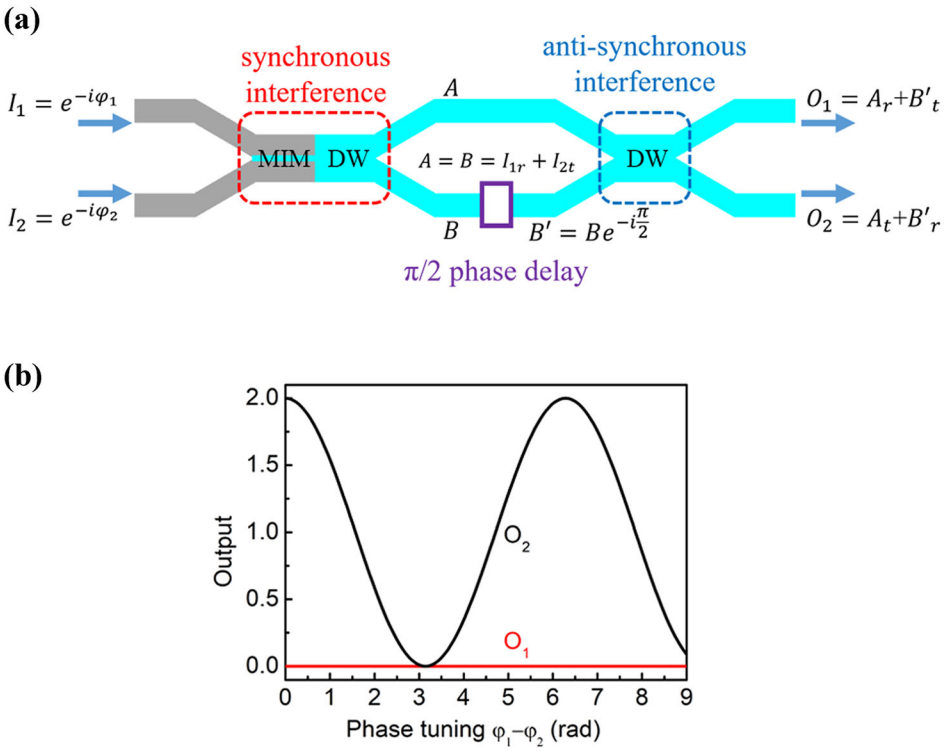

Fig. 3 **a** Scheme of two cascaded systems of synchronous and anti-synchronous interference. **b** Calculation results of the normalized output intensities of O_1 and O_2 (Color figure online)

$$\begin{pmatrix} O_1 \\ O_2 \end{pmatrix} = B_u D B_{nu} \begin{pmatrix} I_1 \\ I_2 \end{pmatrix} = \begin{pmatrix} \frac{\sqrt{2}}{2} & \frac{\sqrt{2}}{2} e^{-i\frac{\pi}{2}} \\ \frac{\sqrt{2}}{2} e^{-i\frac{\pi}{2}} & \frac{\sqrt{2}}{2} \end{pmatrix} \begin{pmatrix} 1 & 0 \\ 0 & e^{i\frac{\pi}{2}} \end{pmatrix} \begin{pmatrix} \alpha & \alpha \\ \alpha & \alpha \end{pmatrix} \begin{pmatrix} I_1 \\ I_2 \end{pmatrix} = \begin{pmatrix} \sqrt{2}\alpha(I_1 + I_2) \\ 0 \end{pmatrix} \tag{3}$$

Typically, the transmission matrix can be given by transmission and reflection coefficients. For non-unitary BS (B_{nu}),$|t| = |r| = \alpha$ owning to the coupling losses and phase difference is zero or π ($t = \pm r$). While for the unitary one (B_u), $|t| = |r| = \frac{\sqrt{2}}{2}$, and the phase difference is $\pm\pi/2$ ($t = \pm ir$). So according to transmission matrix analysis, it is easy to find that one of the outputs keeps a phase-insensitive zero energy state, as shown in Fig. 3b. Moreover, a functional device (i.e., the logic gate XOR) still demands a non-zero output (O_1) with a single input (I_1 or I_2). Fortunately, our previous demonstration of the synchronous interference indicates a directional coupling property. If there is only one input, the single signal passing through the first part will be half-to-half split into two in the next part of the cascade device, resulting in a non-zero output in O_1. If two inputs are excited simultaneously, O_1 will ultimately construct a phase-insensitive output regardless of the input phase differences. So we could possibly construct a phase-insensitive optical logic gate by interference process.

Based on the theoretical analysis, we are going to perform a full-wave simulation. Figure 4a schematically shows the cascaded waveguide design. It should be noted that we use a segment of curved waveguide in one branch of the DW part as a phase retarder to produce $\pi/2$ phase delay. The final interference result is shown in Fig. 4b, where the port O_2 still presents an oscillation feature. In contrast, the port O_1 shows an invariant low intensity that is independent of the input phase tuning, thus indicating a phase-insensitive property. Figure 4c displays the electric field distributions in this phase-insensitive device for three input phase differences of 0, $\pi/2$, and π, respectively. It is clearly demonstrated that the output of O_1 remains at a low intensity all the time, which can be treated as a zero state.

Conclusion

In summary, a cascaded phase-insensitive interference waveguide device is theoretically proposed based on elaborately designed cascaded systems of non-unitary and unitary BSs. An invariant low energy output is achieved independent on the input phase tuning. Compared with the anti-synchronous interference in unitary BS based on a common MMI effect, the non-unitary BS with synchronous

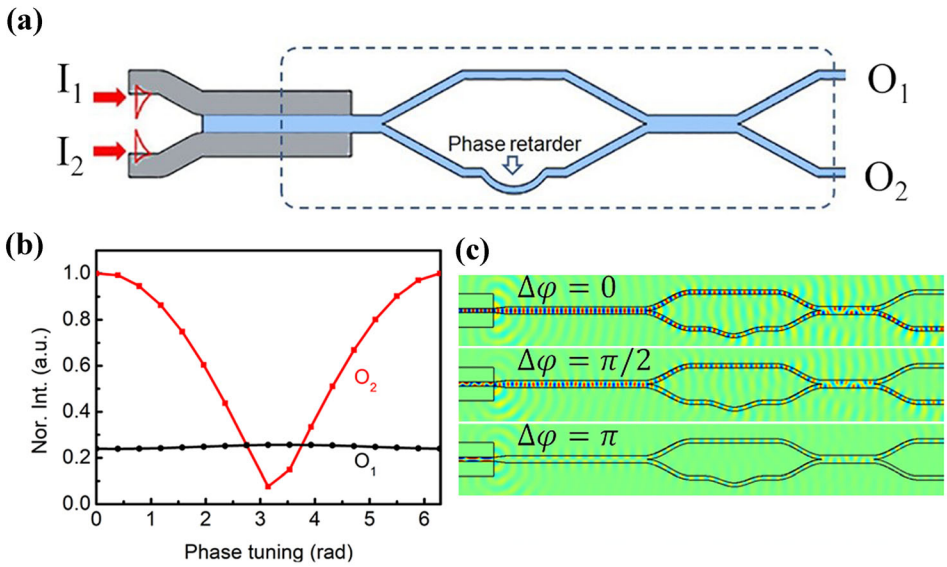

Fig. 4 **a** The schematic structure of the phase-insensitive device. **b** The normalized intensity of the output ports O_1 and O_2 with input phase tuning. **c** The field distributions in the cascaded waveguides with the phase tunings of 0, $\pi/2$, and π

interference is rather difficult to access. Here, we introduce an interface between two segmental waveguides of MIM and DW with well-designed mode properties to satisfy the requirements of synchronous interference and directional coupling property. The full-wave COMSOL simulations show considerably good performance of the phase-insensitive effect. Since the device still has a nonzero output for the single input, which indicates it may work as a phase-insensitive XOR logical gate. Our study discovers an interesting optical process and would possibly inspire more robust optical designs for new types of photonic integrated devices.

Acknowledgements This work was supported by the National Natural Science Foundation of China (NSFC) (Grant No. 11804157). The computational resources generously provided by High Performance Computing Center of Nanjing Tech University are greatly appreciated.

References

1. D. Dai, W. Zhi, J. Peters, J.E. Bowers, Compact polarization beam splitter using an asymmetrical Machczehnder interferometer based on silicon-on-insulator waveguides. IEEE Photon. Technol. Lett. **24**, 673–675 (2012)
2. Y. Xu, J. Xiao, X. Sun, Compact polarization beam splitter for silicon-based slot waveguides using an asymmetrical multimode waveguide. J. Lightw. Technol. **32**, 4884–4890 (2014)
3. Z. Guo, J. Xiao, Ultracompact silicon-based polarization beam splitter using subwavelength gratings. IEEE Photon. Technol. Lett. **29**, 1800–1803 (2017)
4. T. Liu, A.R. Zakharian, M. Fallahi, J.V. Moloney, M. Mansuripur, Design of a compact photonic-crystal-based polarizing beam splitter. IEEE Photon. Technol. Lett. **17**, 1435–1437 (2005)
5. C. He, X. Chen, M. Lu, X. Li, W. Wan, X. Qian, R. Yin, Y. Chen, Tunable one-way cross-waveguide splitter based on gyromagnetic photonic crystal. Appl. Phys. Lett. **96**, 111111 (2010)
6. W. Jia, J. Deng, H. Wu, X. Li, A.J. Danner, Design and fabrication of high-efficiency photonic crystal power beam splitters. Opt. Lett. **36**, 4077–4079 (2011)
7. S.I. Bozhevolnyi, V.S. Volkov, E. Devaux, J.Y. Laluet, T.W. Ebbesen, Channel plasmon subwavelength waveguide components including interferometers and ring resonators. Nature **440**, 508–511 (2006)
8. J.T. Kim, S. Park, Vertical polarization beam splitter using a hybrid long-range surface plasmon polariton waveguide. J. Opt. **16**, 025501 (2014)
9. A.L. Stepanov, J.R. Krenn, H. Ditlbacher, A. Hohenau, A. Drezet, B. Steinberger, A. Leitner, F.R. Aussenegg, Quantitative analysis of surface plasmon interaction with silver nanoparticles. Opt. Lett. **30**, 1524–1526 (2005)
10. F. Gan, C. Sun, H. Li, Q. Gong, J. Chen, On-chip polarization splitter based on a multimode plasmonic waveguide. Photon. Res. **6**, 47–53 (2018)
11. S. Liu, T. Cui, Q. Xu, D. Bao, L. Du, X. Wan, W. Tang, C. Ouyang, X. Zhou, H. Yuan, H. Ma, W. Jiang, J. Han, W. Zhang, Q. Cheng, Anisotropic coding metamaterials and their powerful manipulation of differently polarized terahertz waves. Light: Sci. Appl. **5**, e16076 (2016)
12. O. Wolf, S. Campione, A. Benz, A.P. Ravikumar, S. Liu, T.S. Luk, E.A. Kadlec, E.A. Shaner, J.F. Klem, M.B. Sinclair, I. Brener, Phased-array sources based on nonlinear metamaterial nanocavities. Nat. Commun. **6**, 7667 (2015)
13. P.V. Kapitanova, P. Ginzburg, D.S. Filonov, P.M. Voroshilov, P.A. Belov, A.N. Poddubny, Y.S. Kivshar, G.A. Wurtz, A.V. Zayats, Photonic spin hall effect in hyperbolic metamaterials for polarization-controlled routing of subwavelength modes. Nat. Commun. **5**, 4226 (2014)
14. M. Kim, D. Lee, T.H. Kim, Y. Yang, H.J. Park, J. Rho, Observation of enhanced optical spin hall effect in a vertical hyperbolic metamaterial. ACS Photon. **6**, 2530–2536 (2019)
15. Y. Chen, J. Gu, F. Wang, Y. Cai, Self-splitting properties of a Hermite–Gaussian correlated Schell-model beam. Phys. Rev. A **91**, 013823 (2015)
16. W. Zhu, J. Yu, H. Guan, H. Lu, Z. Chen, Large spatial and angular spin splitting in a thin anisotropic near-zero metamaterial. Opt. Express **25**, 5196 (2017)
17. S. Taravati, A.A. Kishk, Dynamic modulation yields one-way beam splitting. Phys. Rev. B **99**, 075101 (2019)

18. S. Samanta, P.K. Dey, P. Banerji, P. Ganguly, A 1 × 2 polarization-independent power splitter using three-coupled silicon rib waveguides. J. Opt. **20**, 095801 (2018)
19. A. Zeilinger, General properties of lossless beam splitters in interferometry. Am. J. Phys. **49**, 882–883 (1981)
20. V. Degiorgio, Phase shift between the transmitted and the reflected optical fields of a semireflecting lossless mirror is $\pi/2$. Am. J. Phys. **48**, 81–82 (1980)
21. H. Ditlbacher, J.R. Krenn, G. Schider, A. Leitner, F.R. Aussenegg, Two-dimensional optics with surface plasmon polaritons. Appl. Phys. Lett. **81**, 1762–1764 (2002)
22. K. Sun, R.L. Byer, All-reflective Michelson, Sagnac, and Fabryc–Perot interferometers based on grating beam splitters. Opt. Lett. **23**, 567–569 (1998)
23. Z.Y. Ou, J.K. Rhee, L.J. Wang, Observation of four-photon interference with a beam splitter by pulsed parametric down-conversion. Phys. Rev. Lett. **83**, 959–962 (1999)
24. Y.S. Kim, O. Kwon, S.M. Lee, H. Kim, S.K. Choi, H.S. Park, Y.H. Kim, Observation of young's double-slit interference with the three-photon noon state. Opt. Express **19**, 24957–24966 (2011)
25. L. Li, Z. Liu, X. Ren, S. Wang, V.C. Su, M.K. Chen, C.H. Chu, H.Y. Kuo, B. Liu, W. Zang, G. Guo, L. Zhang, Z. Wang, S. Zhu, D.P. Tsai, Metalens-arraycbased high-dimensional and multi-photon quantum source. Science **368**, 1487–1490 (2020)
26. Y. Zhang, K. Wei, F. Xu, Generalized Hong-Ou-Mandel quantum interference with phase-randomized weak coherent states. Phys. Rev. A **101**, 033823 (2020)
27. S. Ding, G. Wang, Extraordinary reflection and transmission with direction dependent wavelength selectivity based on parity-time-symmetric multilayers. J. Appl. Phys. **117**, 31 (2015)
28. H. Fan, J. Chen, Z. Zhao, J. Wen, Y. Huang, Anti-parity-time symmetry in passive nanophotonics. ACS Photon. **7**, 3035–3041 (2020)
29. B. Vest, M.C. Dheur, E. Devaux, A. Baron, E. Rousseau, J.P. Hugonin, J.J. Greffet, G. Messin, F. Marquier, Anti-coalescence of bosons on a lossy beam splitter. Science **356**, 1373–1376 (2017)
30. R. Wen, C. Zou, X. Zhu, P. Chen, Z.Y. Ou, J.F. Chen, W. Zhang, Non-Hermitian magnon-photon interference in an atomic ensemble. Phys. Rev. Lett. **122**, 253602 (2019)
31. Y. Wang, T. Li, L. Wang, H. He, L. Li, Q. Wang, S. Zhu, Plasmonic switch based on composite interference in metallic strip waveguides. Laser Photon. Rev. **8**, 47–51 (2014)
32. L.B. Soldano, E.C.M. Pennings, Optical multi-mode interference devices based on self-imaging: principles and applications. J. Lightw. Technol. **13**, 615–627 (1995)
33. M. Bachmann, P.A. Besse, H. Melchior, General self-imaging properties in $n \times n$ multimode interference couplers including phase relations. Appl. Opt. **33**, 3905–3911 (1994)
34. H. Lu, Z. Cao, H. Li, Q. Shen, Study of ultrahigh-order modes in a symmetrical metal-cladding optical waveguide. Appl. Phys. Lett. **85**, 4579–4581 (2004)
35. A. Panda, P. Sarkar, G. Palai, Studies on coupling of optical power in fiber to semiconductor waveguide at wavelength 1550 nm for photonics integrated circuits. Optik **157**, 944–950 (2018)